A Fiber-Based Master Oscillator Power Amplifier Laser Transmitter for Optical Communications

M. W. Wright[1] and J. Kovalik[1]

To meet the future laser transmitter requirements of deep-space optical communications, a breadboard fiber-based master oscillator power amplifier (MOPA) laser was developed and tested. A polarized output with improved efficiency and higher data rates as compared with previous designs was demonstrated in a modular system. Several source laser configurations were tested and compared along with a programmable pulse-position modulator data encoder. Average powers of up to 10 W at 100 MHz for sub-nanosecond pulses at a 1.06-μm wavelength were measured, extending the previously developed system capability to higher-order pulse-position modulation data formats.

I. Introduction

Pulsed fiber lasers have continued to show significant improvements in performance over the last few years in response to their expanding commercial markets [1]. Their modularity and inherent robustness, as compared with bulk solid-state laser systems, and their scalability from telecommunication systems make it possible for them to be offered as solutions to numerous high-power applications, including free-space optical communications. The laser transmitter development work at the Optical Communications Group at JPL has continued to leverage the commercial development of high-power fiber-based laser master oscillator power amplifier (MOPA) systems along with custom development of the unique modulation components required for pulse-position modulation (PPM) schemes. To this end, we have extended the previous 10-W MOPA system [2] that was capable of pulse repetition frequencies (PRF) of 3 to 30 MHz with 2-ns pulse widths and an overall 9 percent wall-plug efficiency to meet the next-generation requirements for a deep-space optical communications system.

Key points to the new design include polarized beam output and shorter pulse widths to accommodate higher-order PPM formats at increased data rates that require higher peak powers to maintain the link budget. Other features are an increased temporal pulse extinction ratio (ER) to support the use of photon-counting detectors and improved wall-plug efficiency. Pump diode efficiency is the main contributor to the overall efficiency, and much development in the laser community has been focused on this issue in

[1] Communications Architectures and Research Section.

The research described in this publication was carried out by the Jet Propulsion Laboratory, California Institute of Technology, under a contract with the National Aeronautics and Space Administration.

recent years [3,4]. Using a MOPA architecture allows the flexibility of testing separate oscillator or seed lasers with a single high-power amplifier. A directly modulated, high-speed diode was implemented on a custom laser driver board as well as externally modulated continuous wave (CW) seed lasers. The advantage of a directly modulated seed laser is a smaller package and lower system complexity but, as will be shown, it has the potential for degraded performance as compared with an externally modulated seed laser source.

Several lasers were investigated in order to obtain a stable CW source; these included a solid-state Nd:YAG laser, a distributed-fiber Bragg (DFB) grating fiber laser, and a hybrid external-cavity stabilized diode source. The latter two systems proved the most stable and were integrated with the power amplifier stages. No DFB diode lasers were available for testing[2] at 1060 nm, unlike the terrestrial telecommunication wavelength range around 1550 nm. Previous work [2] utilized external-cavity fiber Bragg grating (FBG) fiber-coupled diode lasers that could experience spectral degradation at certain operating points when the device is modulated across a mode hop region.

A modular design was implemented as shown in Fig. 1, with the seed laser, preamplifier, and power amplifier procured commercially while the electronics of the modulator and laser driver along with the data encoder were developed in-house. Section II describes the system design, and the performance of each subsystem is discussed in Section IV. Performance as an integrated system is discussed in Section IV.C.

II. Transmitter Architecture

The performance specifications for the overall system were based on the parameters given in Table 1, mainly driven by the latter power amplifier stage. All the parameters were verified either by the manufacturer or through testing at JPL. The input to the power amplifier stage required an average power of at least approximately 1 mW. Although this power level was possible from the directly modulated seed laser, it could have been challenging for some of the externally modulated seed lasers, especially with lower duty cycles. Hence, a separate fiber preamplifier stage was added to the design. This also allowed the possibility of optical-link field tests with a larger margin of power (up to 0.4 W) than is available with the seed laser alone, but not with the full 10-W output power.

A. PPM Encoder

The previously developed PPM encoder [2] was upgraded with a PC interface. A second compact field-programmable gate array (FPGA)-based board was also built and integrated with the laser driver board for the directly modulated seed laser source, allowing a stand-alone package.

B. Seed Laser—Directly Modulated Diode

As mentioned above, multiple seed laser sources were investigated. The first involved the same FBG fiber-coupled diode laser that was used in the previous system [2] from Lumics, but now it was attached to a custom high-speed laser driver board and integrated with the PPM encoder board. The diode was capable of 150-mW CW output power at 1060 nm with a 30-MHz line width. The laser driver could produce around a 2.5-GHz modulation bandwidth and so was able to support the nanosecond pulses at PRFs up to 100 MHz.

C. Seed Laser—Externally Modulated Lasers

A common device for modulating laser output at high frequencies (>1 GHz) and large extinction ratios (>25 dB) is a Mach–Zender interferometer external modulator. Each arm of the interferometer is an electro-optic crystal whose effective optical path can be changed by applying an external voltage.

[2] DFB sources at 1060 nm have recently become available from Eagleyard Photonics, GBMH, and EM4, Inc.

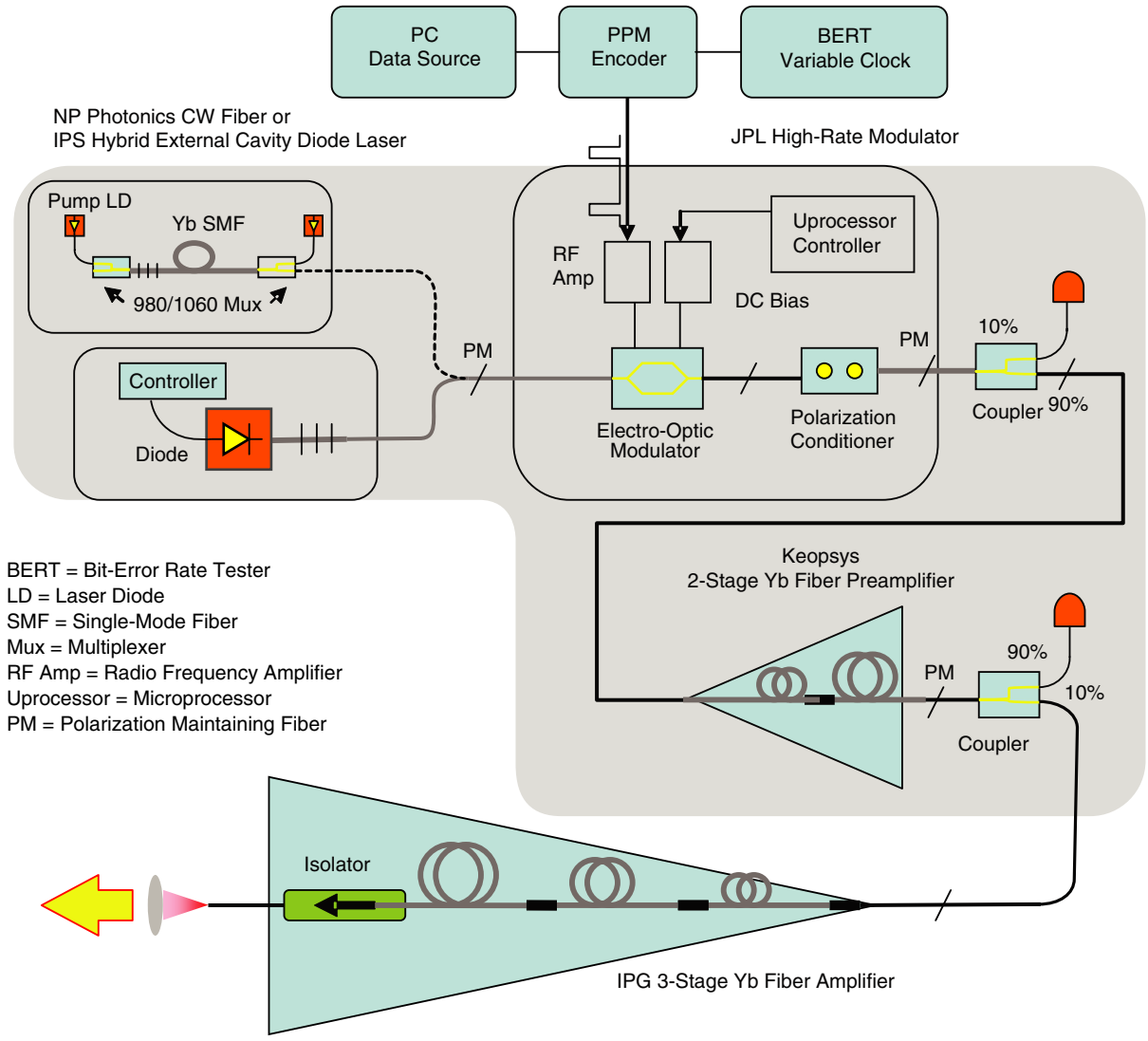

Fig. 1. Schematic of the fiber-based MOPA laser.

By making the relative lengths of the interferometer arms differ by one-half of a wavelength (or 180 deg in phase), the light output of an interferometer port can be completely extinguished. The typical application of these devices is to maintain a dark output and then to create an output light pulse by applying a voltage pulse equal to a half-wavelength path-length difference in one arm (V_π).

Slow changes in the relative path lengths of the interferometer arms caused by temperature drifts, for example, can cause the output of the external modulator to vary over time and move it away from the operating point where the output is dark. Applying a voltage to counteract the path change can eliminate this drift. A standard technique for obtaining the control voltage is to dither the applied voltage by a small amount and then to use a lock in technique to obtain the error signal. In a modified approach used here, the dither signal is applied only intermittently and randomly over time. Since the drifts are typically slow (tens of minutes), the intermittent correction of the drift does not cause a significant change in the extinction ratio. One of the advantages of this technique is that there is no temporally coherent external modulation on the laser output that can confuse clock recovery of PPM signals.

Table 1. Performance requirements.

Parameter	Value
Average output power, P_{avg}	10 W
Repetition rate (PRF)	10–100 MHz
Wavelength, λ_{CL}	<1064 nm
Line width, $\Delta\lambda$	<0.1 nm
Peak power, P_p	>1 kW
Pulse width, τ	≤1 ns
Beam quality, M^2	<1.2
Spatial mode	TEM_{00}
Wall-plug efficiency (including thermal electric cooler)	>15 percent
Extinction ratio (10–100 MHz)	>20 dB, 30 dB desired
Polarization	Linear
Polarization extinction ratio	>17 dB
Energy stability (rms)	<5 percent

These devices are routinely used in telecommunications applications and are packaged in small fiber-coupled modules. Typically, only a few volts are needed to achieve the 180-deg phase shift (V_π). Figure 2 presents a block diagram of the externally modulated laser source. The laser source is a 30-mW CW 1.06-μm diode stabilized by a hybrid external cavity, from Innovative Photonics Solutions (IPS). It is connected to an EOSpace Z-cut lithium niobate 10-gigabits per second (Gbps) external modulator. Other laser sources can be used in this same system by simply switching the input to the modulator. An InGaAS photodiode measures the DC output from the modulator using a 1 percent pickoff and sends the voltage through a digital-to-analog converter (DAC) to a control program on a Rabbit microprocessor. Both the dither signal and the control voltage are also generated by the control program and output by means of a DAC to the DC control input of the modulator. Figure 2 shows a flowchart of the control program.

The program initially goes through a routine in which it sweeps the control voltage over its entire range of −10 V to +10 V and then finds the minimum output. The actual dark output varies with the offset voltage chosen, and this routine finds the optimum one, i.e., the lowest dark current. The program then can be run in various modes, as follows:

(1) A simple DC offset voltage can be applied to the control input of the modulator by means of the Rabbit interface. This simple mode is the equivalent of not using any control system.

(2) The output level can be chosen to vary anywhere from the minimum to the maximum with active control to maintain this level.

(3) The dither and control loop can be run either continuously or at random intervals with the duration and frequency set by the user.

The control loop will work with pulsed output for any duty cycle other than fifty percent. The system minimizes the average output power, and there is no stable minimum operating point when the average power remains one-half of the maximum, since this corresponds to both a dark and bright fringe for the interferometer output.

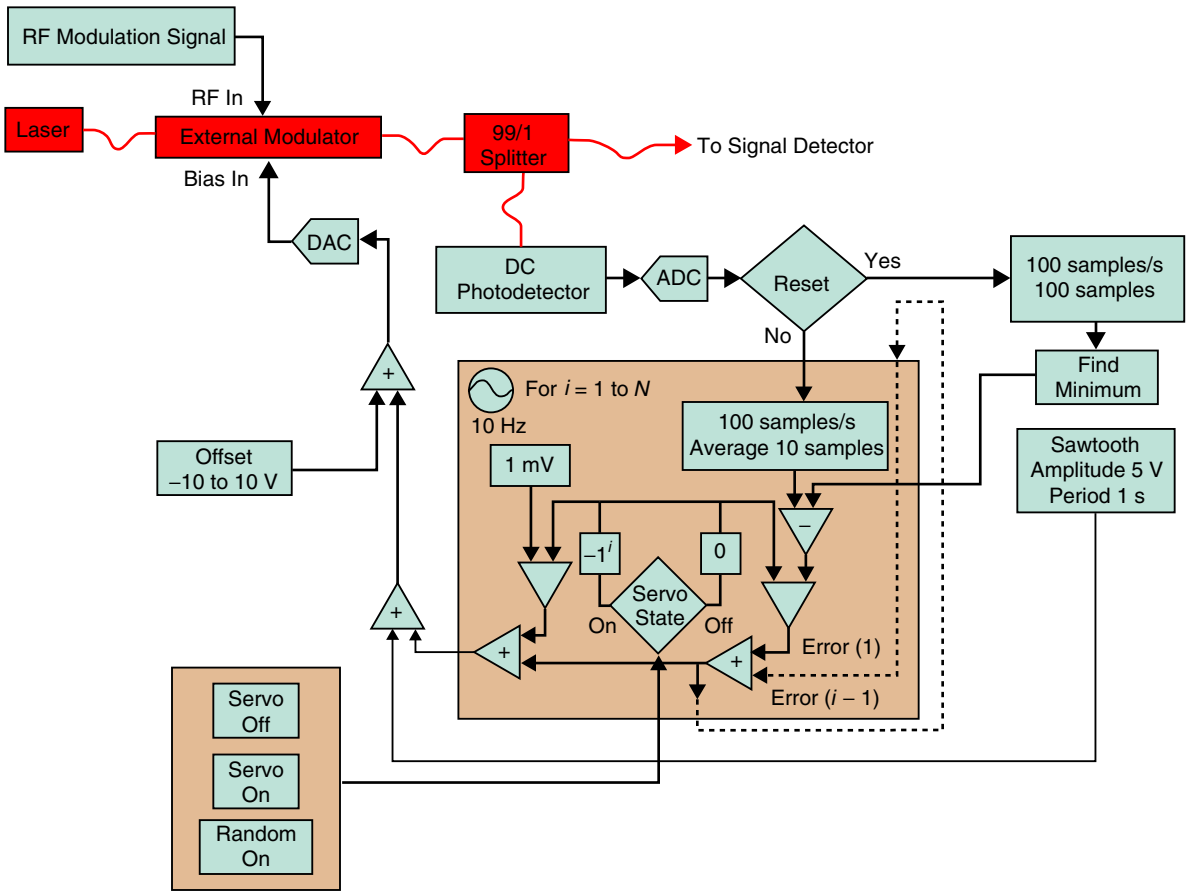

Fig. 2. Block diagram for the externally modulated laser seed source.

D. Preamplifier

The specifications of the fiber preamplifier are listed in Table 2. The system was developed by Keopsys, Inc., and included a two-stage design with mid-stage isolation and control through an RS-232 port. Total signal gain was on the order of 37 dB with a 2-nm bandpass filter mid-stage.

E. Amplifier

The system specifications outlined in Table 1 were met by the final fiber amplifier developed by IPG Photonics, Inc. It involved a three-stage Yb-doped dual-clad fiber amplifier design with spectral filters between each stage to limit the amplified spontaneous emission (ASE) buildup. The fiber-coupled pump diodes had a nominal 50 percent electrical–optical efficiency out of the fiber.

III. Experiment

The system was set-up with 90/10 fiber tap couplers between each stage to monitor the signal as it is propagated though the amplifier chain. Power measurements were made with either a thermal power meter or an optical power meter at low power levels. Pulse width and extinction ratio (ER) measurements used a 1- or 1.5-GHz bandwidth detector initially and checked with a 5-GHz PIN diode on a 1.5-GHz Agilent digitizing oscilloscope. The ER measurements were obtained by expanding the scope scale to derive the "off" pulse voltage. Maximizing the peak power may yield more accurate values [5] for lower duty cycles. The spectra were recorded on an optical signal analyzer (OSA) with 0.01-nm resolution. The clock output of a bit-error rate tester was used for the variable clock source for the PPM encoder.

Table 2. Preamplifier specifications.

Parameter	Value
Average output power, P_{avg}	>300 mW
Optical input power	>100 μW
Operating wavelength, λ_{CL}	1064 ± 5 nm
Maximum output peak power, P_p	300 W (100 ps at 10 MHz)
Input pulse width, τ	100–500 ps
Polarization	Linear
Polarization extinction ratio	>20 dB
Output beam quality	Single mode

IV. Results

A. Seed Laser Characterization

Initially an Nd:YAG laser from Crystal Laser was proposed as the CW seed source due to its spectral purity and low noise as compared with diode sources. The device was heat-sunk to the optical table with an enclosure to limit temperature variations from the laboratory environment. However, preliminary data showed a root-mean-square (rms) variation of power of ∼1 percent/hour, as shown in Fig. 3, after a 40-minute warm-up time. Wavelength stability was good at <0.003 percent/hour, as was the polarization extinction ratio (PER) of 30 dB, measured by monitoring the power after rotating a broadband polarizing beam-splitter cube in the output beam.

A fiber laser from NP Photonics with integrated fiber Bragg gratings for wavelength control also was tested along with another CW source, the hybrid external-cavity diode laser from IPS. The latter provided excellent power and wavelength stability, as shown in Fig. 4, with less than 0.2 percent variation per hour and low relative intensity noise. Although both of these systems were integrated in two separate chassis, only the latter will be reported on here. The lasers were single mode with line widths on the order of kilohertz, beyond the OSA resolution.

Figure 5 shows the stability performance of the external modulator servo system. The DC power output of the laser is measured in five different ways. The first two are standard configurations of the laser manufacturer: current and power control modes. The DC power output is also measured with the modulator servo set to maintain the intensity at 80 percent of the maximum possible intensity. Three different configurations are used:

(1) Servo on: The servo is always on.

(2) Servo 4 s: Turn on the servo for 0.1 s at a random point in time during every 4-s interval.

(3) Servo 60 s: Turn on the servo for 0.1 s at a random point in time during every 60-s interval.

Figure 6 shows an enlargement of the measurements for the servoed system. It is clear that the DC laser stability is improved by the servo and that greater stability is obtained for more frequent application of the servo.

The directly modulated diode laser was tested at various PRFs (Fig. 7) and shows reasonable pulse–pulse stability, as shown in Fig. 7(b). Representative spectra are shown in Fig. 7(c), along with output

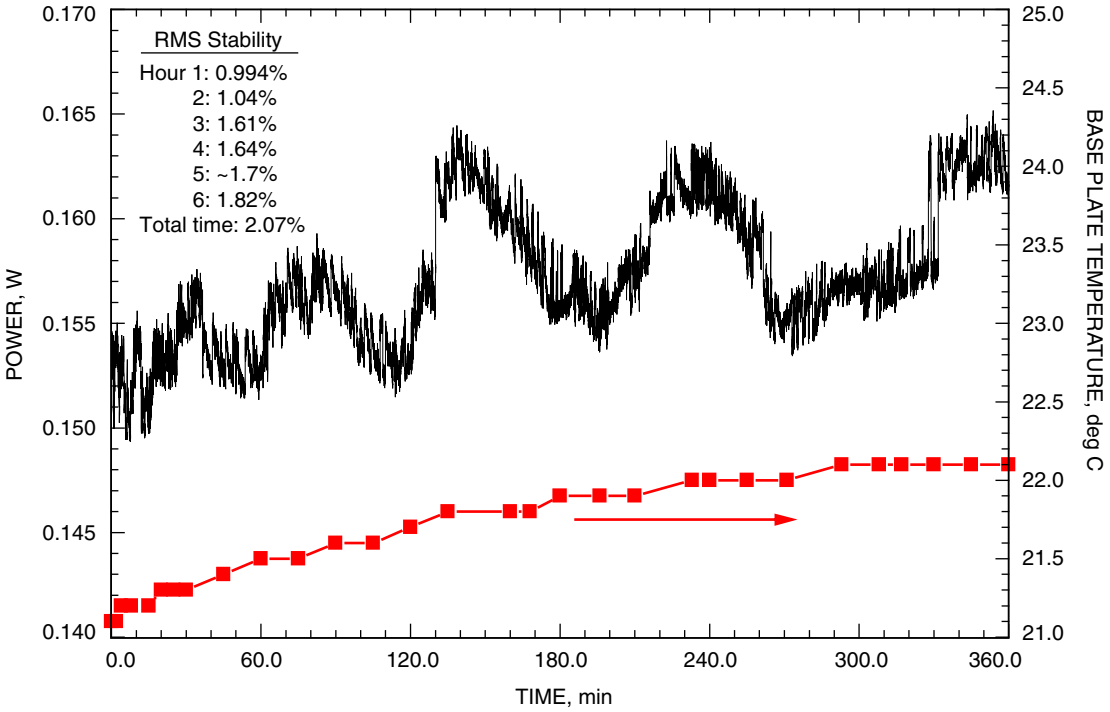

Fig. 3. Nd:YAG power stability over 6 hours.

power as a function of PRF in Fig. 7(a). Biasing the device near threshold at 33 mA gave narrower pulse widths and increased pulse peak intensities as compared with biasing slightly above threshold. Although only slightly visible in the seed laser pulse data (Fig. 8), the increased emission in the off state becomes greatly exaggerated under amplification (see later in Section IV.C). Pulse widths were nominally the same over the range of PRFs with a full width at half maximum (FWHM) of 0.9 ns near threshold, increasing to 1.5 ns for $I_{\text{bias}} = 35$ mA. It is critical to operate at the optimum bias point to limit the emission in the off state and increase the energy per pulse.

B. Preamplifier Characterization

The CW output power of the preamplifier is shown in Fig. 9(a), along with the spectra, Fig. 9(b), at high power and for several input powers, Fig. 9(c). With an externally modulated input, the time-averaged pulsed output spectra are shown in Fig. 9(d). The optical signal-to-noise ratio (OSNR) was measured for a given spectral bandpass and plotted in Fig. 10 as a function of the input seed laser power using a CW diode as the source. The 2-nm bandpass represents the mid-stage filter in the preamplifier.

C. System Characterization with Amplifier

With an average input power of around 1 mW, the amplifier output power and spectrum with an externally modulated input seed laser are shown in Fig. 11. Slight pulse broadening from 1 to 1.25 ns was seen at high power. Figure 12 shows pulsed time spectra for fixed repetition rates using a variable duty cycle pulse train that covered the range of PRFs specified for the system. Figure 13 plots the relative pulse energy as a function of spectral bandpass for various repetition rates. The variable duty cycle case closely follows the lower repetition rate, with slight spectral broadening. The ERs are given in Table 3. With direct diode modulation for the seed source, ERs up to 39 dB were possible prior to amplification by optimizing the bias and modulation currents. However, after amplification, the measured ERs were still consistent with those in Table 3. For fixed repetition rates, the ERs were within experimental error of those for the variable duty cycle cases but typically decreased for higher repetition rates. Externally modulated fiber lasers [6] have shown ER > 35 dB, but these use two-stage cascaded modulators.

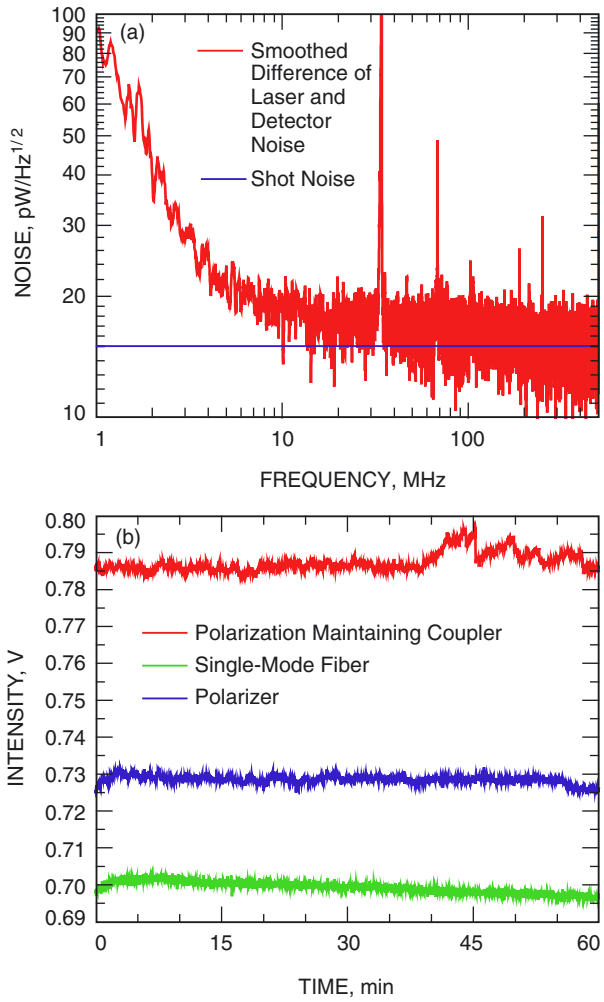

Fig. 4. Hybrid laser stability data: (a) noise spectra and (b) temporal spectra.

The OSNR was slightly degraded for the directly modulated seed laser, as can also be seen in the spectra of Fig. 14(a). As the seed diode is biased above threshold, the ASE is reduced significantly at the lower PRFs, where higher peak powers are present. At the higher PRFs, Fig. 14(b), no discernible difference can be seen by adjusting the seed laser bias point. Again, the variable duty cycle case, Fig. 14(c), follows the low PRF situation. Measuring pulse energy directly is challenging due to the narrow pulses and convolved detector response function. However, a relative measure can be seen by comparing the peak heights of the time spectra for various PRFs. Figures 15 and 16 compare the pulse heights for various seed laser bias points at moderate output power for a fixed PRF and a variable duty cycle. In both cases, there is nearly a factor of two increase in peak power as the seed laser is biased close to threshold as compared with that above threshold. Although the pulse width also broadens from 0.86 ns at threshold to 1.25 ns above threshold, it is not enough to compensate the increased peak power. Taking into account the higher ER as well, it follows then that higher pulse energies are obtained with broader spectral width for the seed laser biased near threshold. Some of the increased energy would then go into the pedestal of the laser line. To obtain a measure of this, the relative spectral power density is plotted in Fig. 17 from the spectra. Although more energetic pulses are obtained when the seed laser is biased

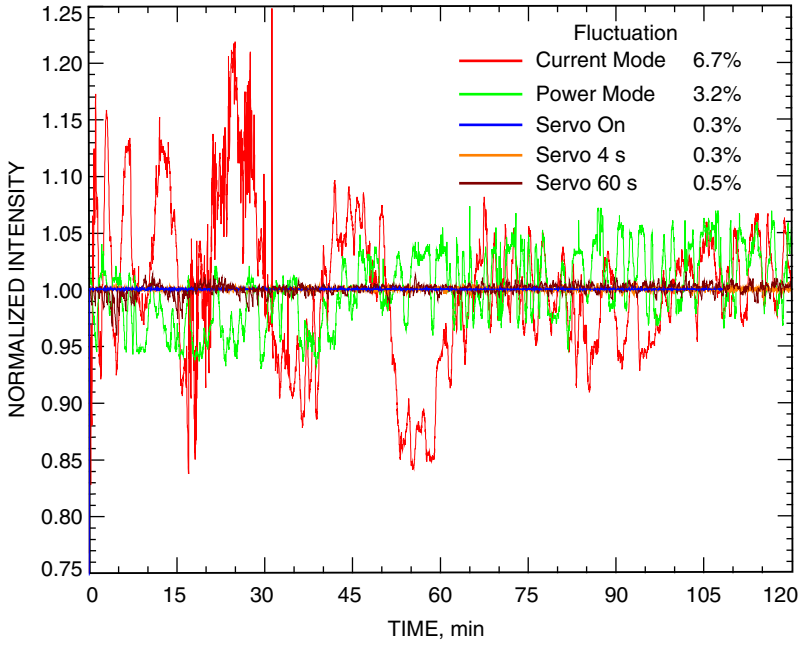

Fig. 5. Laser DC power output stability for different configurations of the externally modulated seed laser.

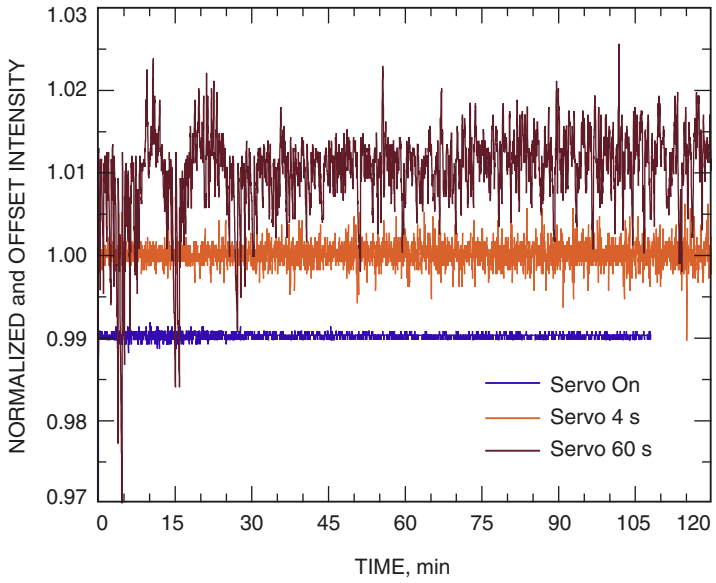

Fig. 6. Performance of the servoed system in the externally modulated seed laser using different time durations for application of the servo.

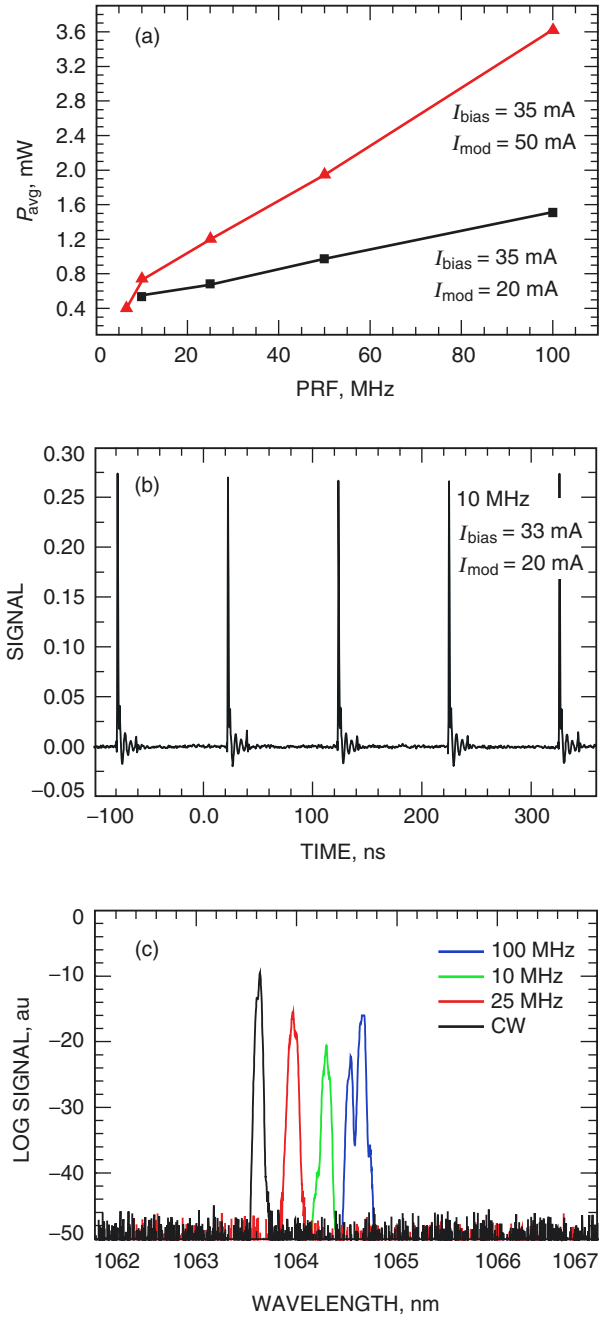

Fig. 7. Seed laser output: (a) average power as a function of repetition rate for two modulation currents, (b) time spectra, and (c) wavelength spectra under pulsed and CW conditions, offset for clarity.

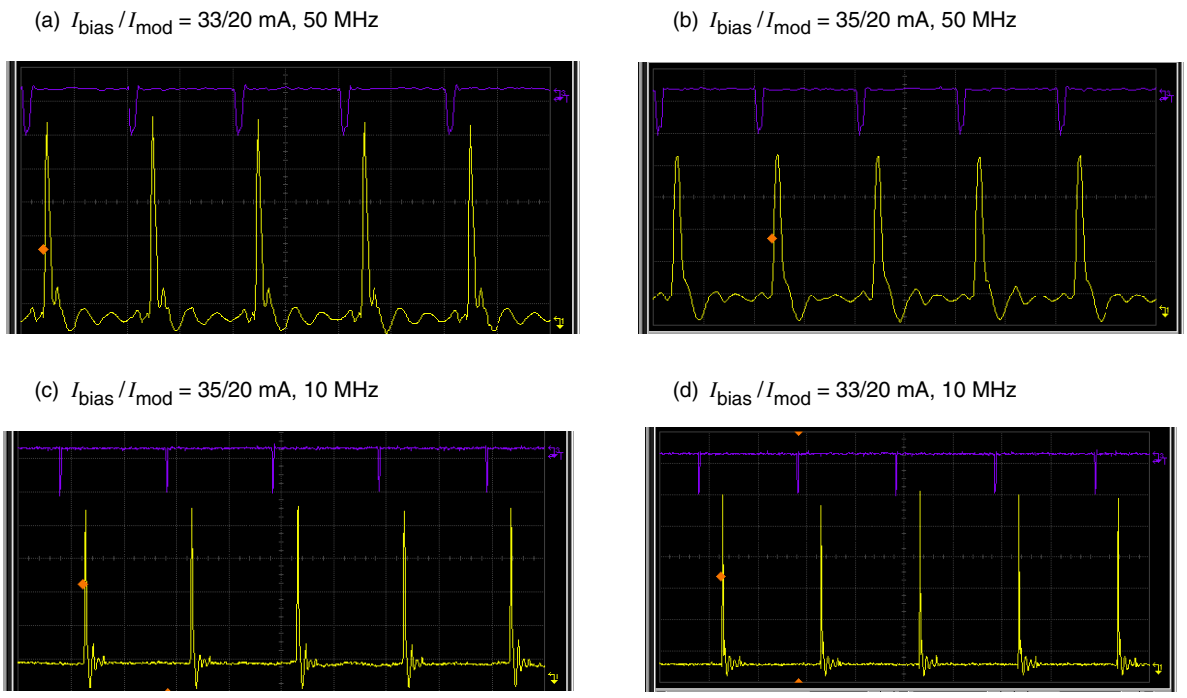

Fig. 8. Seed laser time trace with bias values of (a) 33 mA and (b) 35 mA at 50 MHz and of (c) 35 mA and (d) 33 mA at 10 MHz. The top curve in each graph is the inverted RF input with a 10-ns/division scale for 50 MHz and a 50-ns/division scale for the 10-MHz data. The vertical scale is the same for all cases.

near threshold, there is an increase in power outside of the laser line. In a typical receiver, to improve the signal-to-noise ratio, a narrowband filter is placed around the laser line. This would have the effect of decreasing the signal power when the seed laser is biased near threshold. To obtain high pulse energy in a narrow spectral width, these two competing effects, high peak power with high ER and a broadened laser line, must be traded to optimize the communication performance of a directly modulated seed laser system.

It was also noted that, under variable duty cycles, the pulse energies as measured by the peak heights were consistent within experimental uncertainty, as desired for any transmitter. This points to the lack of gain depletion in the amplifier, even under the maximum variable duty cycle that the laser would see for the given data formats.

The amplifier could also be operated without the fiber preamplifier and fed directly from the diode laser source. No significant difference was seen in the output characteristics as compared with the directly modulated diode and the preamplified input.

Power efficiency measurements were made by noting the pump diode currents. The indicated pump diode current was actually applied only to the current draw of a second bank of pump diodes. The first bank of pump diodes was set to a nominal value to ensure adequate amplifier saturation at turn-on. For the amplifier alone, an overall wall-plug efficiency of 17 percent was possible at high power output.

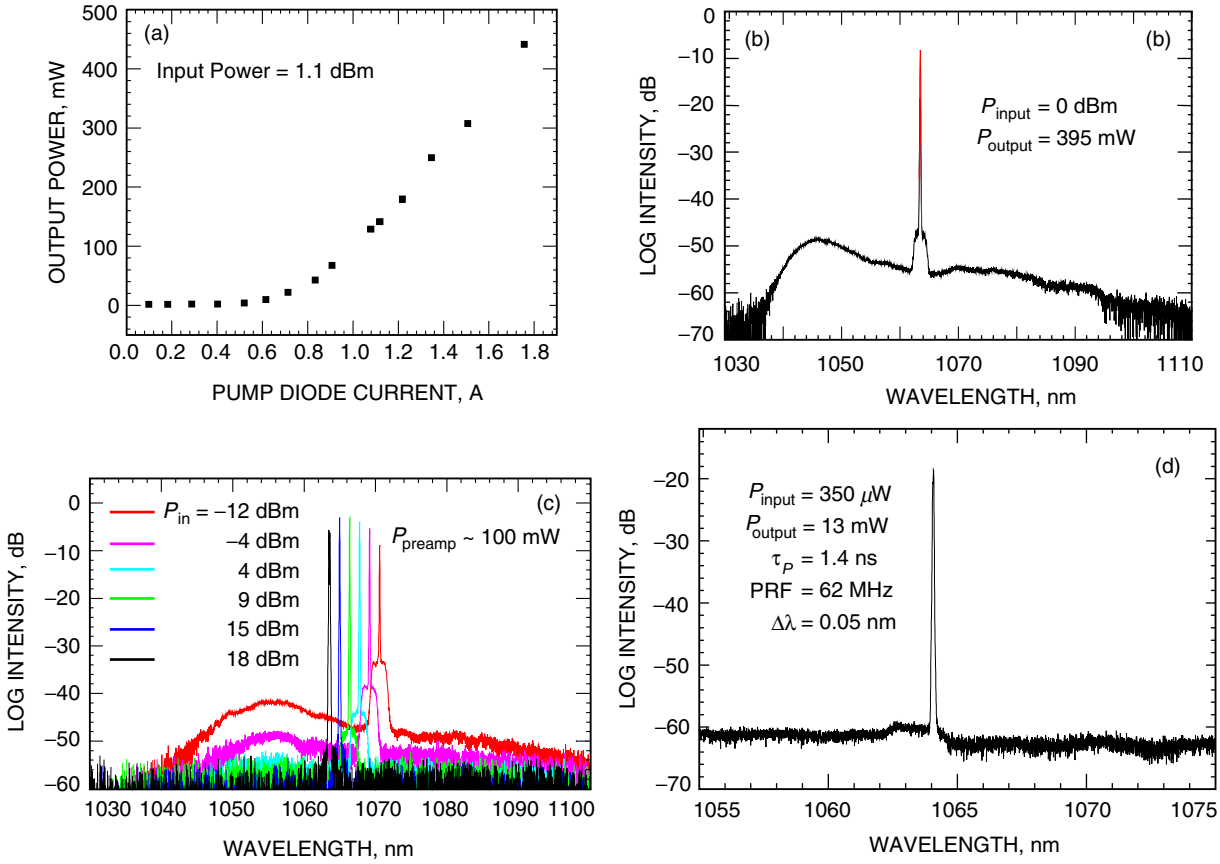

Fig. 9. Preamplifier data: (a) output power with CW input, (b) spectra at high power, (c) spectra for varying input powers, and (d) output spectra at low power with externally modulated input.

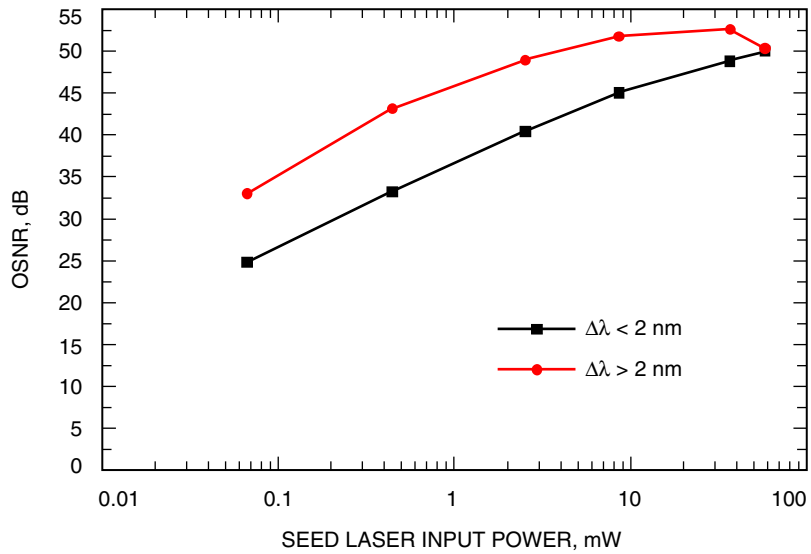

Fig. 10. Optical SNR of the preamplifier output with CW input.

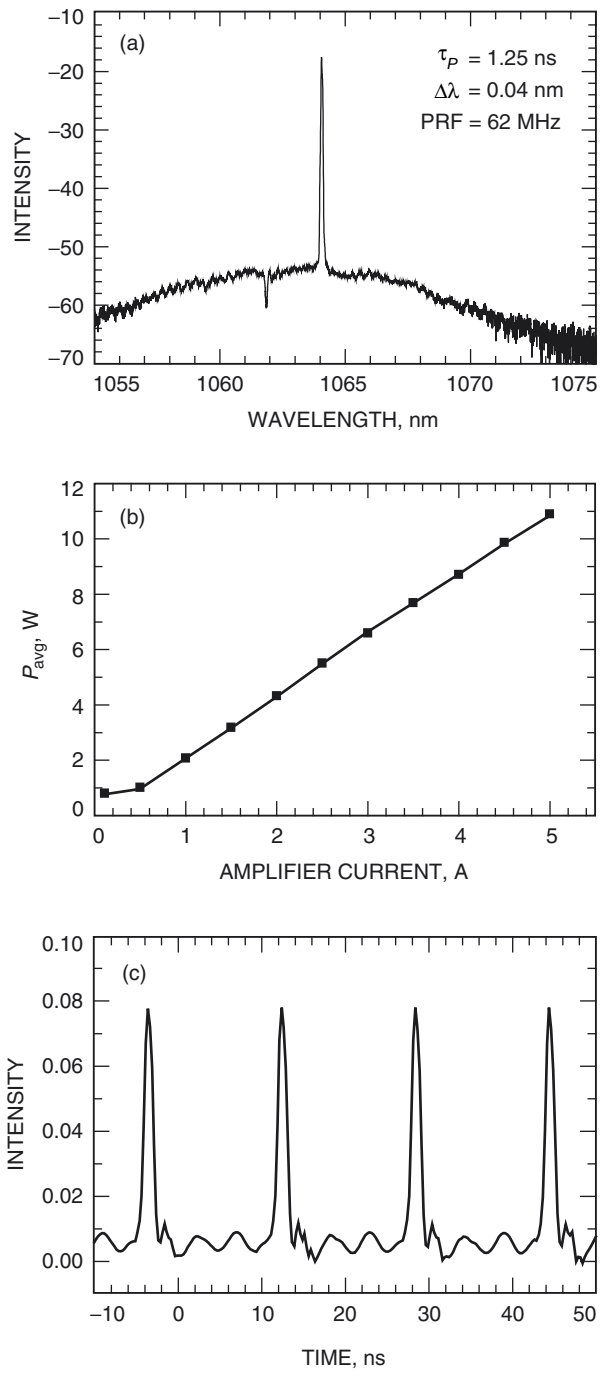

Fig. 11. Amplifier output with preamplifier and externally modulated fiber laser seed: (a) spectra at 10-W average output power and PRF = 62 MHz, (b) average output power as a function of pump laser current, and (c) pulsed time spectra at 10-W average output power.

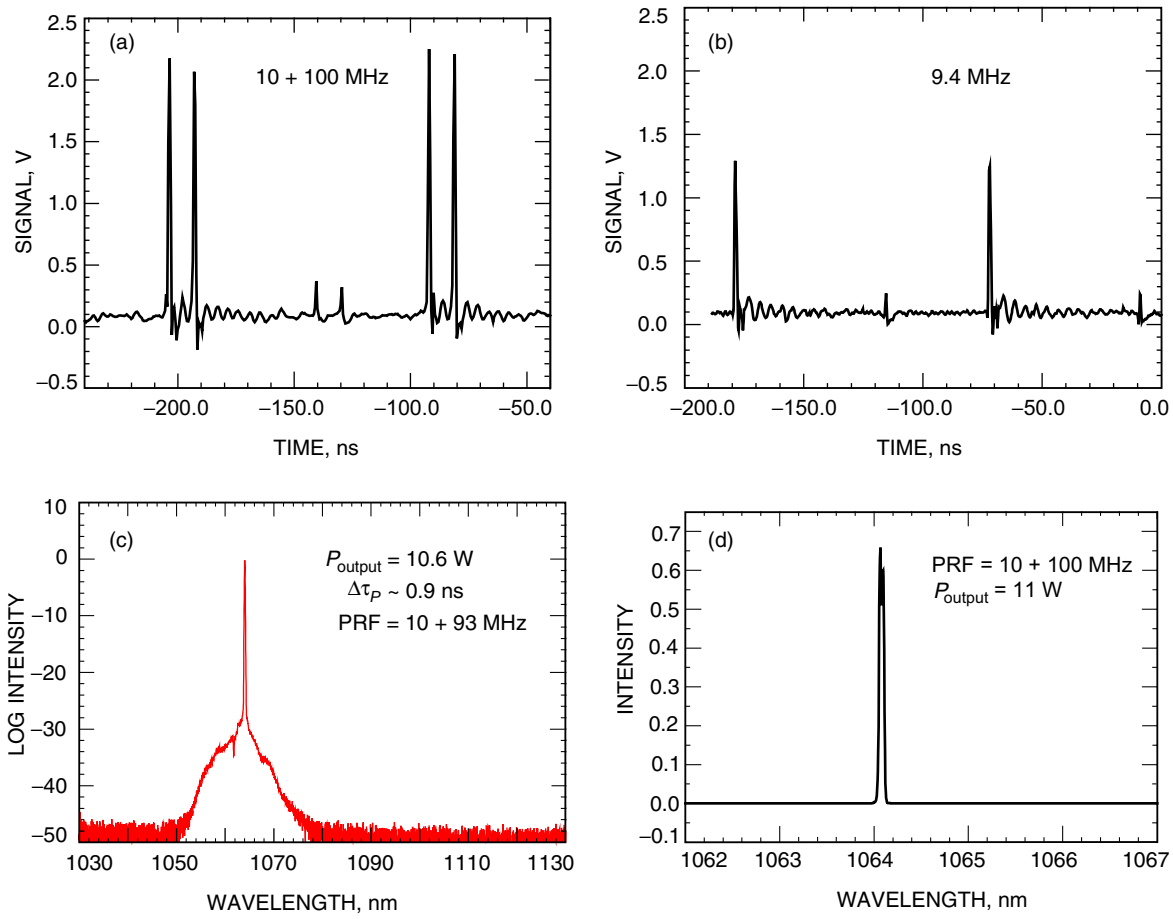

Fig. 12. Amplifier output at 11-W average power and externally modulated seed laser: time spectra with (a) a variable duty cycle and (b) a fixed repetition rate input; output spectra on (c) log and (d) linear scales, with variable duty cycle pulsed input.

V. Discussion

In comparing the externally modulated and the directly modulated seed lasers, operating points can be found for both cases that give optimum communication performance where high pulse energy, narrow spectral width, and high ER could be achieved. For instance, if the optical link budget requires a 0.1-nm bandpass filter for the receiver, a directly modulated seed laser needs to be biased above threshold, and the amplifier power must be increased to increase the pulse energy. Alternatively, an externally modulated seed laser could be used with an increased amplifier power to compensate the broadened spectral line width.

For long-range optical communications where low signal detection levels are required, PPM data formats are more efficient than on–off keying (OOK). This format lends itself well to maximum-likelihood codes with photon-counting detectors that are baselined for such systems. The current laser system allows for a PPM order of 64 when slot widths and hence pulse widths of just under 1 ns are used. If the pulse widths can be furthered reduced to 0.4 ns, higher PPM orders such as 128 or more may be possible. Peak power typically limits the amplifiers. However, no non-linearities were evident in the output spectra in the present operating range, suggesting there is some margin in the data rates. In fact, shorter pulsed

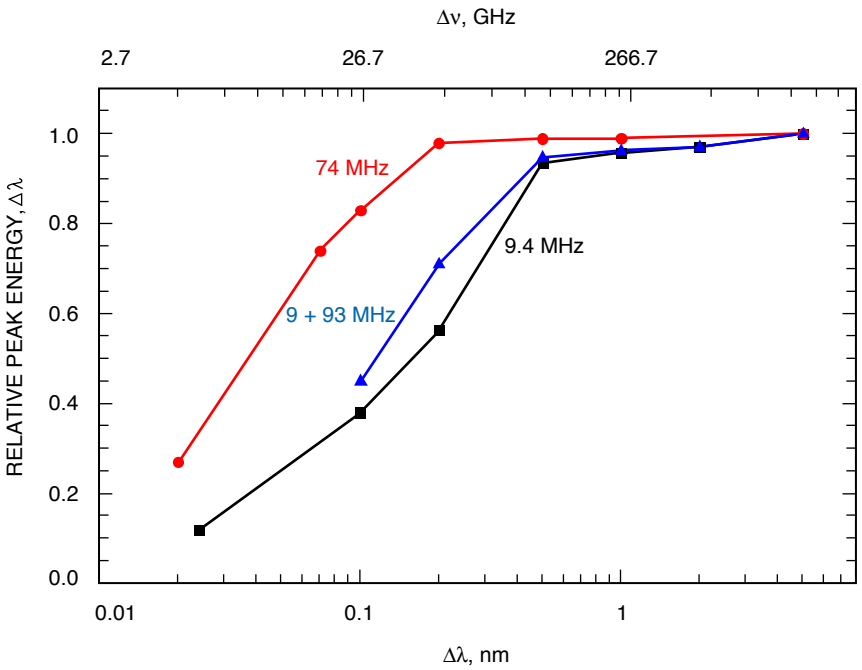

Fig. 13. Relative pulse energy of the amplifier output as a function of spectral bandpass for various repetition rates. The amplifier was set at 10.6-W average output power and had a pulse width of 0.9 ns with an externally modulated seed laser.

Table 3. ER measurements for the 10 + 100 MHz variable duty cycle case.

Source	ER, dB
Externally modulated—seed only	21.5
Externally modulated—amplifier, 10.2 W	20.1
Directly modulated—seed only, $I_b/I_m = 33/50$ mA	27
Directly modulated—seed only, $I_b/I_m = 35/50$ mA	20.5
Directly modulated—amplifier, 10 W (33/50 mA)	26.3
Directly modulated—amplifier, 10 W (35/50 mA)	19

operation with 100-ps pulse widths was demonstrated with the current device, but this will be reported elsewhere. Higher data rates are limited by the high-speed electronics of the seed laser and reduced amplifier pulse energies. Future systems would incorporate these narrow pulse widths for high data rates as well as address the component reliability without sacrificing overall efficiency.

VI. Conclusion

A second-generation fiber MOPA laser was developed and tested as a breadboard optical communications transmitter. The device was capable of nanosecond pulses at up to a 100-MHz repetition rate in a polarized output beam with an integrated data encoder. Such a system could support PPM data formats up to order 64, or even 128 with narrower seed pulses, for link ranges over deep-space distances.

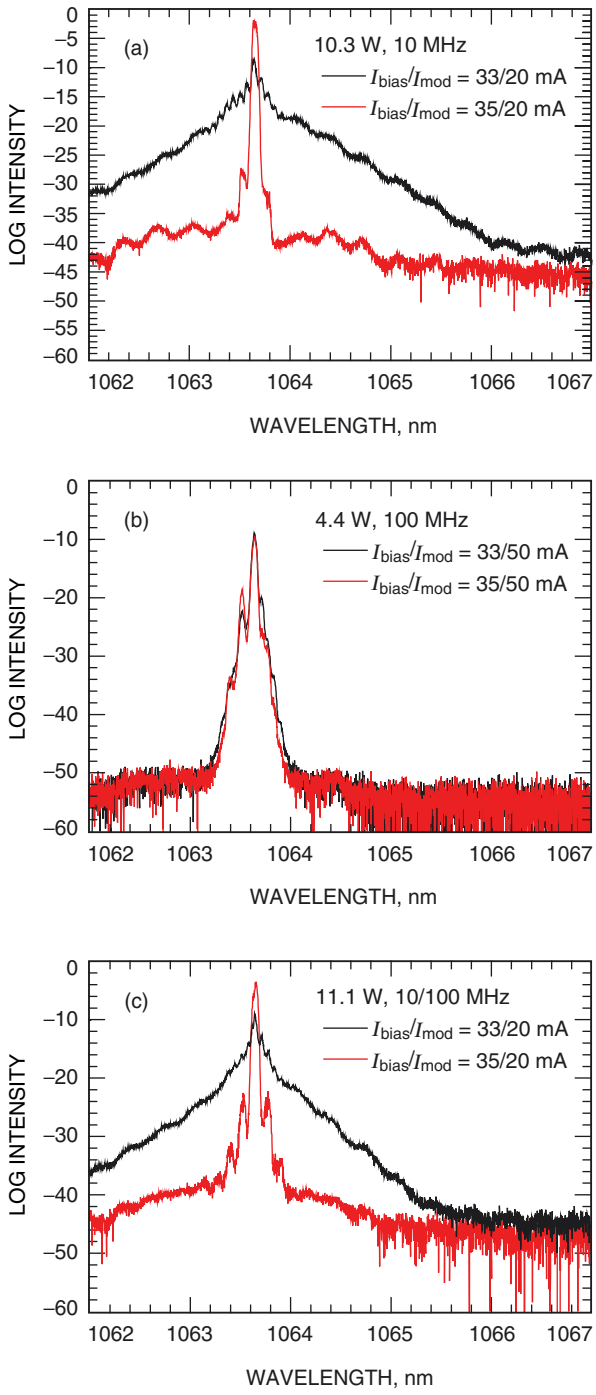

Fig. 14. Amplifier output with directly modulated seed laser imput biased at threshold (33 mA) and just above threshold (35 mA): (a) 10.3 W at PRF = 10 MHz, (b) 4.4 W at 100 MHz, and (c) 11.1 W with a variable duty cycle corresponding to 10 and 100 MHz.

(a) I_{bias} / I_{mod} = 35/50 mA

(b) I_{bias} / I_{mod} = 33/50 mA

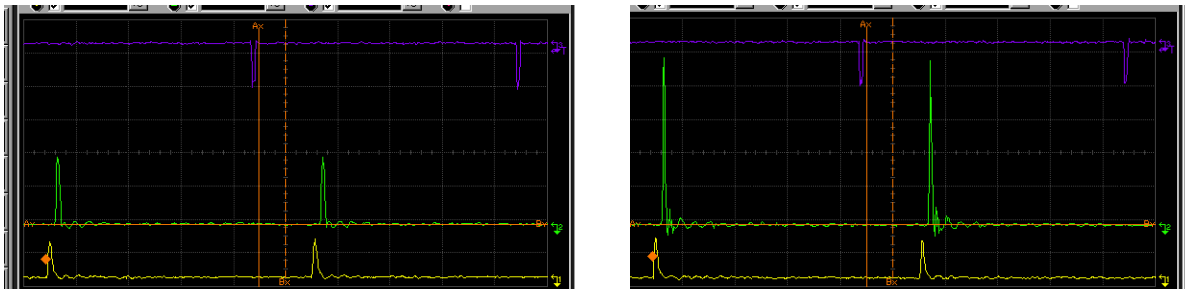

Fig. 15. The amplifier output with a preamplifier and a directly modulated seed laser at a fixed repetition rate of 10 MHz and 4.3 W. The upper traces are the inverted trigger, the lower traces are the input signal, and the middle traces are the amplifier output: (a) biased above threshold and (b) biased at threshold.

(a) I_{bias} / I_{mod} = 35/50 mA

(b) I_{bias} / I_{mod} = 33/50 mA

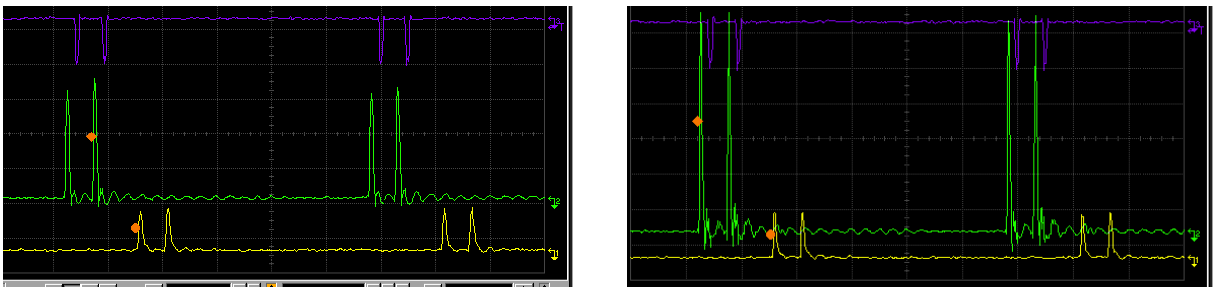

Fig. 16. The amplifier with a preamplifier and a directly modulated seed laser at variable duty cycles corresponding to 10 and 100 MHz and 4-W average output power. The upper traces are the trigger, the lower traces are the input signal, and the middle traces are the amplifier output: (a) biased above threshold (mean pulse width ~ 1.25 ns) and (b) biased at threshold (mean pulse width ~ 0.864 ns).

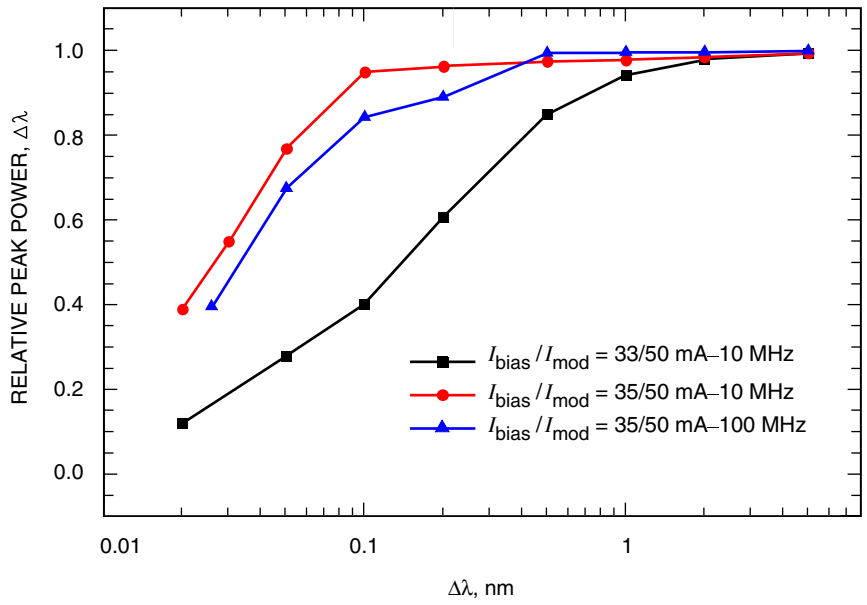

Fig. 17. Relative peak power as a function of spectral width for the amplifier at 4.3 W, with a preamplifier and directly modulated seed laser input.

References

[1] B. Shiner, "High-Power Fiber Lasers Gain Market Share," *Industrial Laser Solutions*, vol. 21, no. 2, 2006.

[2] M. W. Wright, D. Zhu, and W. Farr, "Characterization of a High-Power Fiber Master Oscillator Power Amplifier (MOPA) as an Optical Communications Transmitter," *The Interplanetary Network Progress Report*, vol. 42-161, Jet Propulsion Laboratory, Pasadena, California, pp. 1–12, May 15, 2005. http://ipnpr/progress_report/42-161/161F.pdf

[3] M. Peters, V. Rossin, M. Everett, and E. Zucker, "High Power, High Efficiency Laser Diodes at JDSU," *Proceedings of the SPIE*, vol. 6456, 64560G, 2007.

[4] P. Crump, W. Dong, M. Grimshaw, J. Wang, S. Patterson, D. Wise, M. DeFranza, S. Elim, S. Zhang, M. Bougher, J. Patterson, S. Das, J. Bell, J. Farmer, M. DeVito, and R. Martinsen, "100-W+ Diode Laser Bars Show >71% Power Conversion from 790-nm to 1000-nm and Have Clear Route to >85%," *Proceedings of the SPIE*, vol. 6456, 64560M, 2007.

[5] D. O. Caplan, "A Technique for Measuring and Optimizing Modulator Extinction Ratio," *CLEO*, pp. 335–336, May 10, 2000.

[6] N. W. Spellmeyer, D. O. Caplan, B. S. Robinson, D. Sandberg, M. L. Stevens, M. M. Willis, D. V. Gapontsev, N. S. Platonov, and A. Yusim, "A High-Efficiency Ytterbium-Doped Fiber Amplifier Designed for Interplanetary Laser Communications," OFC/NFOEC Meeting, Paper OMF2, Anaheim, California, March 25–29, 2007.